

# Paleofluid flow: answers in the quartz.

Kevin Freville (✉ [kevin.freville@gmail.com](mailto:kevin.freville@gmail.com))

Université d'Orléans <https://orcid.org/0000-0002-1569-7467>

Stanislas Sizaret

Université d'Orléans

---

## Article

**Keywords:** Hydrothermalism, geothermy, fluid flow, numerical modeling, Limagne Basin

**Posted Date:** April 12th, 2021

**DOI:** <https://doi.org/10.21203/rs.3.rs-403809/v1>

**License:**   This work is licensed under a Creative Commons Attribution 4.0 International License.

[Read Full License](#)

---

# Abstract

The search for carbon-free energy sources is at the heart of our concerns. It has become necessary to develop our capacities to harness the active energy flows of our environment while trying to have the lowest possible impact. Among these flows, one of the most stable is that linked to terrestrial thermal anomalies. Geothermal energy is an attractive option due to its regularity and the development of knowledge is encouraged, in France, by the national research funding agency. Geothermal systems are mainly associated with active hydrothermal circulations, fluids can be considered as a source of heat but also of metals. However, fluid circulation within active hydrothermal fields occurs at considerable depths and cannot be observed directly. In this study we propose a method for reconstructing the paleo-flow velocities recorded by quartz. The relative thickness of quartz growth bands is used to deduce the sense and velocity of the paleofluid flow. This contribution highlights the paleofluid flows velocities and the recharge/discharge area in the Limagne Basin geothermal province, which is currently under investigation. Finally, this study provides a tool to be used to study fossil hydrothermal systems containing quartz veins with comb textures.

## Introduction

Resources related to hydrothermal systems are numerous: active “hot water” fields are exploited for energy production, moreover many fossil systems may have metal concentrations of economic interest<sup>1,2</sup>. Increasing the precision of the targets for geological exploration is one of the new challenges for society. It will enable and direct low-impact investigations leading to new sources for our energy and metal needs in the coming years. The identification of recharge and discharge areas, and the identification of flows by the alterations and/or the deformations they cause are the prime parameters for understanding hydrothermal systems<sup>3</sup>. Currently, knowledge of the flows in these systems is provided by numerical modeling based on petrophysical properties (porosity, permeability)<sup>4,5</sup>. These computed solutions are strongly dependent on local geometries and permeability, with fluctuation over several orders of magnitude. The direct identification of paleoflows from field information is possible, but remains marginal in publications from the 1940s<sup>6–8</sup>. Recent studies have investigated mineralized paleo hydrothermal systems rich in tourmaline<sup>9,10</sup>. This work proposes to reconstruct the paleocirculation in the fossil portions of a geothermal field being explored currently. The method is based on the one developed for tourmaline<sup>11</sup> but here applied to quartz: an ubiquitous vein-filling mineral. The objective of this study is to provide a useful tool for deciphering paleohydrodynamics, based on a real example.

## Methods

***Main concept, to use quartz growth to decipher hydrodynamics.***

The starting point of the method is to consider the thicknesses of the growth bands in minerals as the materialization of an integrated chemical flow during a short period of time<sup>11</sup>. For crystallographically equivalent faces, when the kinetics of the surface process are fast, the differences in thickness of the

growth bands are controlled by the flow of the fluid medium<sup>10,12</sup>. The latter can be related to a local concentration gradient and to flow speed<sup>9-11,13</sup>. This last hypothesis constitutes the framework of our study, and we defend the following two propositions.

The first is the use of variations in the thicknesses of the growth bands of equivalent faces to deduce a direction of flow<sup>6</sup>. For equivalent crystal surface properties, the largest thickness is facing the upstream flow while the thinner is less fed in the downstream position. In quartz, the sections perpendicular to the axis <c> make it possible to compare the thicknesses of the growth bands of equivalent faces on the same crystal<sup>6-8</sup>. Two borderline cases appear in which the symmetries of flow and crystal overlap. The first is the case where the leading edge of the fluid is on a ridge. The fluid velocity vector then makes, apparently, an angle of 30° with the two upstream and downstream faces of the section. A velocity vector perpendicular to the upstream face constitutes the second case. The majority of the geometries are intermediate and the reconstitution of the direction of flow must be evaluated by an operator. This proposition was discussed for quartz in the 1940s and more recently for tourmaline<sup>6,13</sup>. However, the use of this method has remained very marginal until today.

The second proposition consists in deducing the flow velocity of the fluid from the ratio of the thicknesses of the upstream and downstream growth bands. The approach consists in numerically modeling the chemical fluxes of crystal growth and determining the variation of the flux ratio as a function of the upstream speed. Ultimately the speed of the fluid will be deduced by the inverse method by calculating the ratio of the thicknesses of the growth bands and by comparing this value to the  $V_{\text{fluid}}$  curve versus the ratio of fluxes (Figure 1). The models show that the flow ratios also depend, and mainly, on the geometry of the crystal, the angle of incidence between the speed and the growth faces, and the size of the crystal. It is therefore advisable to model the curve with a geometry as close as possible to that observed. In the case of quartz, we have considered two modes of growth, the first, very common, is growth on the trigonal prism, and the second mode on the faces of the basal prism.

The figure 1 synthesizes the results, the 715 simulations are presented in the attached materials. Obviously all the ratios increase with velocity until a maximum velocity value and then decrease. After the maximum, for high velocities, the curve is interrupted because the boundary layer is detached downstream the crystal and produces turbulences. In this area the turbulent regime re-homogenizes the concentration in the boundary layer and produce a decrease of the flux ratio. The position of this maximum is strongly dependent on the grain size: small grains are able to record high velocity flows whereas large ones record low velocities (Figure 1B). The quantitative estimation of the flow velocity is also strongly influenced by the incidence angle between the flow direction and the crystal face. In the case of flow perpendicular to the upstream face, on the same crystal two different ratios exist relative to the upstream and downstream face respectively (Figure. 1B). The higher ratio corresponds to the downstream faces. The velocities calculated from such “upstream” or “downstream” ratios may vary by one order of magnitude. In the case of a flow with a symmetrical incident angle giving a symmetrical situation, obviously the ratios are equivalent. Thus, the definition of the fluid flow direction necessitates a

priori the calculation of the growth band ratio for each face of the crystal. In the same way, the ratio calculated in 3D for a trigonal pyramid's growth shows a similar evolution. The estimations of flow velocities based on equivalent faces of a trigonal pyramid could change the ratio by more than one order of magnitude in comparison with the basal growth model. Finally, our results show that both the temperature of the fluids and changes in the face size have negligible effects on relative growth rate of equivalent faces (Figure 1B and supplementary material).

## Results

### *Geological setting*

Located in the northern portion of the French Massif Central, the Limagne Basin consists of a hemi-graben filled with Tertiary sedimentary rocks such as arkoses, sandstones and conglomerates<sup>14,15</sup> (Figure 2). Three main normal faults can be distinguished separating the Tertiary sediments and the Variscan basement, which is composed of Variscan granitoids and metamorphic rocks. Some Quaternary basalt flow can also be observed (Figure 2B). The Eastern fault and the SW-NE Aigueperse fault meet at the N-S Clermont Ferrand Fault (Figure 2B)<sup>16</sup>. This basin is also characterized by the presence of numerous CO<sub>2</sub>-rich thermomineral waters with high temperature springs reaching 33° C at the surface, indicating fluid circulation<sup>17</sup>. Five years ago, Calcagno et al.<sup>18</sup> identified a good geothermal potential for the basin, based on its thermal anomaly.

Outcrops at the boundary between the basement and the cover show quartz veins indicating the initial stages of the functioning of this hydrothermal field (Figure 3A). Sites where the vein density was highest were assumed to represent singular points in terms of hydrothermal recharge/discharge of the basin. Overall, the veins observed are sub-vertical with fillings of comb-textured quartz. On the western border vein orientations of N90-120E dominate whereas on the eastern edge, the directions are from N90E to N25E; finally, in the south the orientations are around N25E.

### *Fluid flow within the Limagne basin:*

The estimation of fluid flow velocity must be based upon the growth mode. Most of the comb quartz crystals observed in longitudinal section by C-L image display pyramidal growth (Figures 1B, 3B). We also note some crystals with prismatic growth (Figures 1A, 3B). However, it was found that most of the quartz crystals formed exhibit a pyramidal growth mode (i.e., *r* face) and that the *m* (prismatic) face grows only passively<sup>19</sup>. Nevertheless, in our case, taken from nature, in some cases we observe growth along the *m* face.

In order to compare equivalent faces, we prepared thin sections perpendicular to the *c* axis of the quartz grains, in the case of comb-textured quartz this means parallel to the vein wall (Figure 1C). Here, we consider that the main growing mode is on the trigonal pyramid; however, in both cases the thickest growth band, on the opposite face from the thinnest gives the hydrothermal flow direction (Figure 1). A

single quartz grains may record more than one flow direction during its crystallization, which can be in the upward, downward or lateral direction (Figure 1C).

Accordingly, in our work we have deduced the velocities of the fluid flow for both growth modes. In the eastern part of the basin (Sans-Soucis area, Figure 2B) we find a downward flow reaching  $10^{-6}$  to  $10^{-4}$  m.s<sup>-1</sup> when considering the prismatic growth, and  $10^{-7}$  to  $10^{-5}$  m.s<sup>-1</sup> for the pyramid (Figures 2D,E, 4). Within the Charbonière-les-Varennes area, we observe firstly a downward fluid flow, followed by a lateral flow direction with a large range of fluid flow velocities from  $10^{-7}$  to  $10^{-4}$  m.s<sup>-1</sup> or less when using the pyramidal growth mode (Figure 4). To the south, in the Roure area, we record only a lateral fluid flow with velocities of ca.  $10^{-6}$  to  $10^{-5}$  m.s<sup>-1</sup> or  $10^{-6}$  to  $10^{-7}$  m.s<sup>-1</sup> (Figure 2E,D, ; 4). As for the Southern region, the Ris area records a mainly lateral flow with a wide range of fluid flow velocities of ca.  $10^{-6}$  to  $10^{-3}$  m.s<sup>-1</sup> (Figure 2 E,D; 4). We also note the presence of quartz grains with no asymmetry in the growth bands, indicating a low velocity fluid flow. Moreover, lower velocities are recorded for the downward flow. Here, we can see that the flow is discontinuous over time and changes in velocity and direction.

## Discussion Of The Hydrothermal System Of The Limagne Basin, And Conclusions

We have used the quartz-hydrothermal mineralization in veins to identify the paleo- recharge/discharge area and the associated fluid flows. The asymmetric growth of equivalent quartz crystal faces has enabled us to define the direction of the paleofluid flow responsible for forming these quartz veins. The method, when applied to the whole Limagne Basin, allows the recharge and discharge areas to be identified. The flow is discontinuous over time and changes in velocity and direction, but in a continuous tectonic setting. A first downward flow of  $10^{-6}$  to  $10^{-3}$  m.s<sup>-1</sup> corresponding to the recharge area has been identified close to the thermal anomaly. However, the location of the recharge area is in disagreement with the earlier model, under which the fault zone intersection is where fluid flow is classically supposed to be upward<sup>22</sup>. A second mainly lateral flow of  $10^{-6}$  to  $10^{-4}$  m.s<sup>-1</sup> has been found in all other parts of the Limagne Basin, and corresponds to the discharge areas. (Figure 2).

We obtain relatively high fluid flow velocities in comparison with the fluid flow velocities calculated in numerous numerical modelings ( $10^{-14}$  to  $10^{-7}$  m.s<sup>-1</sup>)<sup>4,5</sup>. Such a difference in this velocity's value may be explained by the fluid's circulation functioning in short pulses, whereas in the numerical modeling the fluid flow is continuous and averaged in time and space. The conceptual fault valve model is now widely discussed in the literature. It describes a cycle of increased overpressure and tectonic stresses released during earthquakes. It results in a rapid change in the pressure gradient and therefore in the direction of flow of fluids<sup>20,21</sup>. Finally, this study on quartz provides to the scientific community with a method for on-site investigations of the paleo hydrodynamics of fossil hydrothermal systems.

## Declarations

## ACKNOWLEDGEMENT

This work was conducted in the framework of the REFLET project (French National Research Agency grant agreement No. ANR\_10-IEED-0802-02 which is supported by the French Government through the Investments for the Future programmes. We strongly appreciate the English review of this contribution from J.V. Guy-Bray.

## References

1. Hurter, S. & Schellschmidt, R. Atlas of geothermal resources in Europe. *Geothermics* **32**, 779–787 (2003).
2. Kanazawa, Y. & Kamitani, M. Rare earth minerals and resources in the world. *J. Alloys Compd.* **408–412**, 1339–1343 (2006).
3. Cloetingh, S. *et al.* Lithosphere tectonics and thermo-mechanical properties: An integrated modelling approach for Enhanced Geothermal Systems exploration in Europe. *Earth-Sci. Rev.* **102**, 159–206 (2010).
4. Guillou-Frottier, L., Carré, C., Bourguin, B., Bouchot, V. & Genter, A. Structure of hydrothermal convection in the Upper Rhine Graben as inferred from corrected temperature data and basin-scale numerical models. *J. Volcanol. Geotherm. Res.* **256**, 29–49 (2013).
5. Taillefer, A. *et al.* Fault-Related Controls on Upward Hydrothermal Flow: An Integrated Geological Study of the Têt Fault System, Eastern Pyrénées (France). *Geofluids* **2017**, 1–19 (2017).
6. Newhouse, W. H. The direction of flow of mineralizing solutions. *Econ. Geol.* **36**, 612–629 (1941).
7. Engel, A. E. J. The quartz crystal deposits of western arkansas. *Econ. Geol.* **41**, 598–618 (1946).
8. Engel, A. E. J. The direction of flow of mineralizing solutions. *Econ. Geol.* **43**, 655–660 (1948).
9. Sizaret, S. *et al.* Estimating the local paleo-fluid flow velocity: New textural method and application to metasomatism. *Earth Planet. Sci. Lett.* **280**, 71–82 (2009).
10. Sizaret, S., Fedioun, I., Barbanson, L. & Chen, Y. Crystallization in flow - II. Modelling crystal growth kinetics controlled by boundary layer thickness. *Geophys. J. Int.* **167**, 1027–1034 (2006).
11. Sizaret, S. *et al.* Crystallisation in flow Part I: paleo-circulation track by texture analysis and magnetic fabrics. *Geophys. J. Int.* **167**, 605–612 (2006).
12. Gilmer, G. H., Ghez, R. & Cabrera, N. An analysis of combined surface and volume diffusion processes in crystal growth. *J. Cryst. Growth* **8**, 79–93 (1971).
13. Launay, G., Sizaret, S., Guillou-Frottier, L., Gloaguen, E. & Pinto, F. Deciphering fluid flow at the magmatic-hydrothermal transition: A case study from the world-class Panasqueira W–Sn–(Cu) ore deposit (Portugal). *Earth Planet. Sci. Lett.* **499**, 1–12 (2018).
14. Morange, A., Heritier, F. & Villemin, J. Contribution de l'exploration pétrolière à la connaissance structurale et sédimentaire de la Limagne, dans le Massif Central. in *Symposium Jung J, Clermont Ferrand* (1971).

15. Autran, A. *et al.* Les sédiments post-paléozoïques. *Rev Sci Nat Auver* **45**, 69–74 (1979).
16. Michon, L. Dynamique de l'extension continentale - Application au Rift Ouest-Européen par l'étude de la province du Massif Central. (Université Blaise Pascal - Clermont-Ferrand II, 2000).
17. Martelet, G., Bitri, A., Guillou-Frottier, L., Perrin, J. & Serrano, O. *Méthodologie de l'inventaire géothermique de la Limagne: projet COPGEN. Compilation des données géophysiques.* (2003).
18. Calcagno, P., Baujard, C., Guillou-Frottier, L., Dagallier, A. & Genter, A. Estimation of the deep geothermal potential within the Tertiary Limagne basin (French Massif Central): An integrated 3D geological and thermal approach. *Geothermics* **51**, 496–508 (2014).
19. Kleshchev, G. V., Bryzgalov, A. N., Chernyi, L. N., Kuznetsov, A. F. & Nikitichev, P. I. Some Trends in Shape Production for Artificial Quartz Crystals. in *Growth of Crystals* (ed. Sheftal', N. N.) 147–153 (Springer US, 1976). doi:10.1007/978-1-4613-4256-4\_11.
20. Sibson, R. H. Tectonic controls on maximum sustainable overpressure: fluid redistribution from stress transitions. *J. Geochem. Explor.* **69–70**, 471–475 (2000).
21. Passelègue, François. X., Brantut, N. & Mitchell, T. M. Fault Reactivation by Fluid Injection: Controls From Stress State and Injection Rate. *Geophys. Res. Lett.* **45**, (2018).
22. Faulds, J. E. & Hinz, N. H. Favorable Tectonic and Structural Settings of Geothermal Systems in the Great Basin Region, Western USA: Proxies for Discovering Blind Geothermal Systems. *Proc. World Geotherm. Congr.* (2015).

## Figures

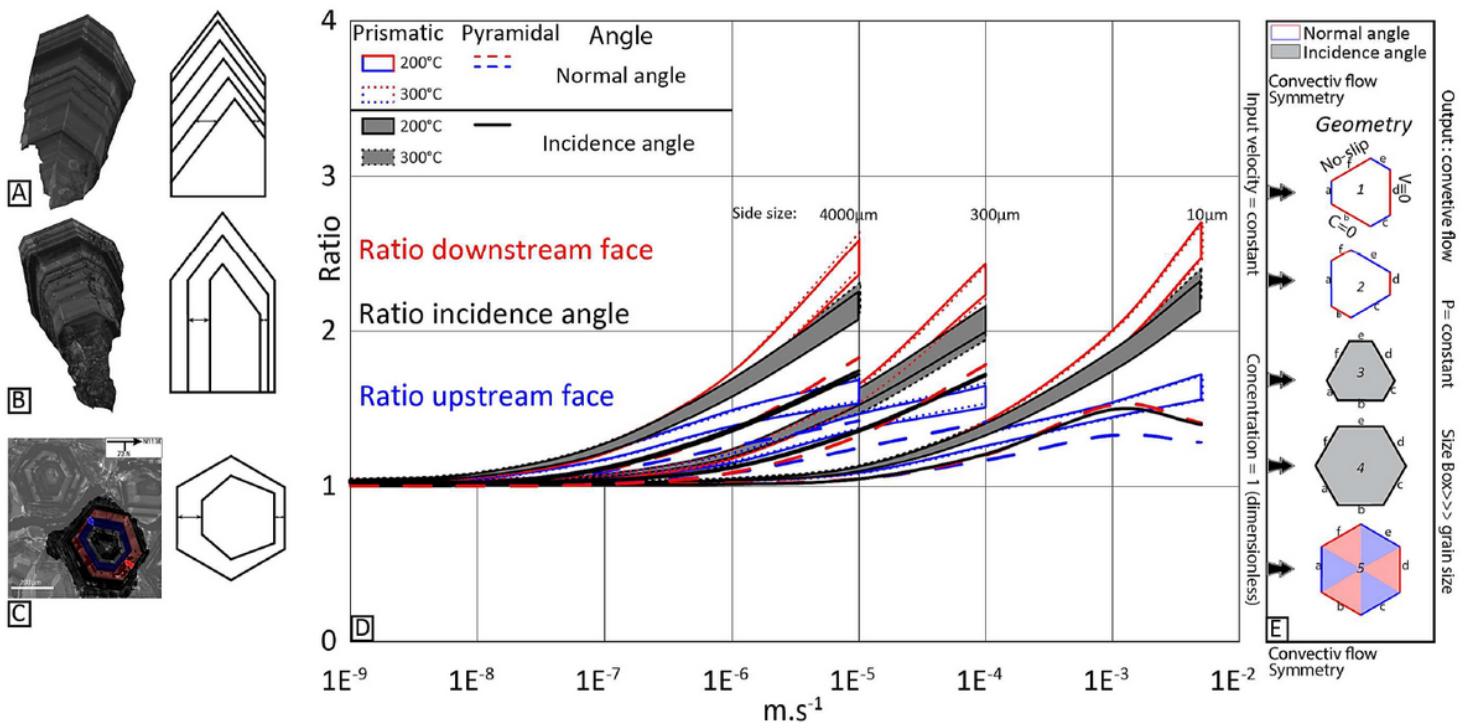
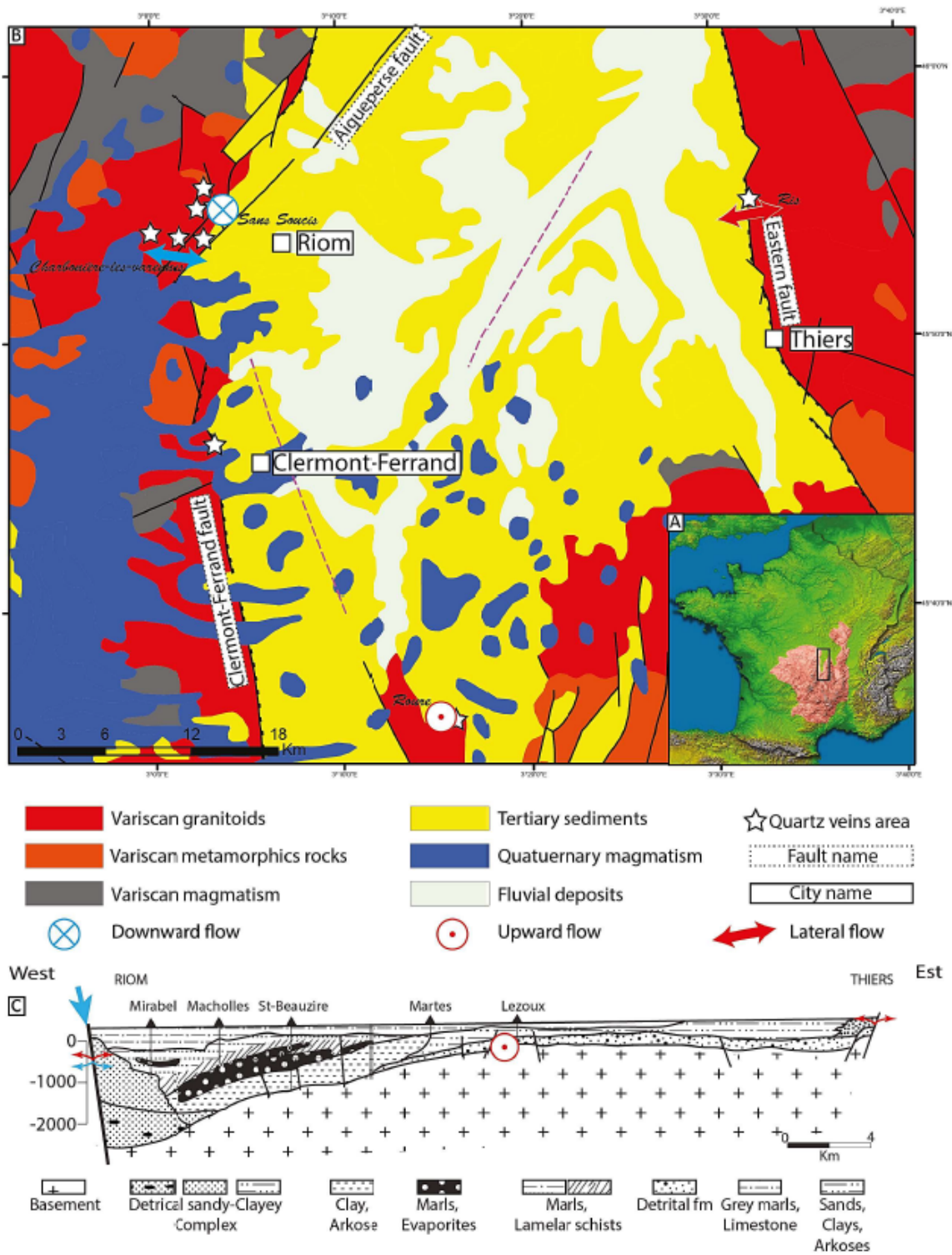


Figure 1

A. Cathodoluminescence photomicrograph of quartz grain growing along the trigonal pyramid faces (r face) B. Cathodoluminescence photomicrograph of quartz grain growing along the faces parallel to the c-axis (m face) C. Cathodoluminescence photomicrograph of a quartz grain showing the growth bands. Red and blue arrows indicate the respective directions of the downstream and upstream flows. D. Synthesis of fluid flow models. In the case of a flow perpendicular to the prismatic upstream face: red boxed curve represents the ratio for the “downstream” face ratio (faces: b-d-f) and blue boxed curve represents the ratio for the “upstream” face ratio (faces: a-c-e). Grey boxed curve represents ratio for a geometry with a symmetrical situation for the faces a-c-e and f-b-d. The red dotted line represents the ratio for the “downstream” face ratio (b-d-f) and the blue dotted line represents the ratio of the “upstream” face ratio (a-c-e) in pyramidal growing mode for a geometry with a normal angle. The black line represents the ratio for a geometry with a symmetrical situation. E. Geometry of quartz grains used for the simulation. 3D (Pyramidal) models have been made with the geometry 4 and 5.





**Figure 2**

A. Location of the Limagne Basin (French Massif Central). B. Simplified geological map of the Limagne Basin showing the sample locations and the fluid flow circulation. C. Geological cross-section of the Limagne hemi-graben<sup>14,15</sup>.



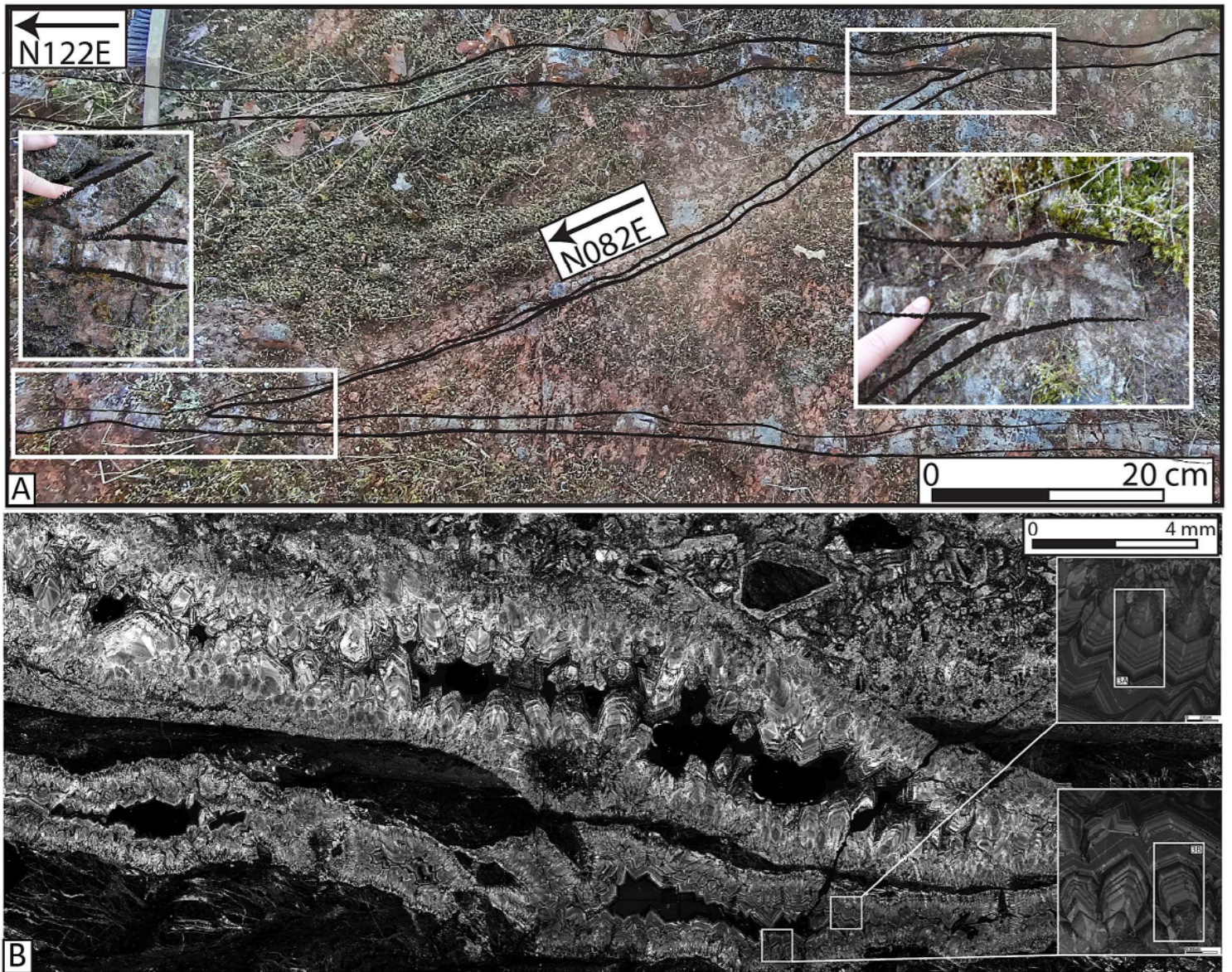


**Figure 3**

A. Outcrop photograph of anastomosing comb-quartz veins. B. Cathodoluminescence photomicrograph of quartz veins and details. C. Stereographic diagram of poles of quartz veins plotted on the lower hemisphere in equal-area-projection for both side of the Limagne Basin.

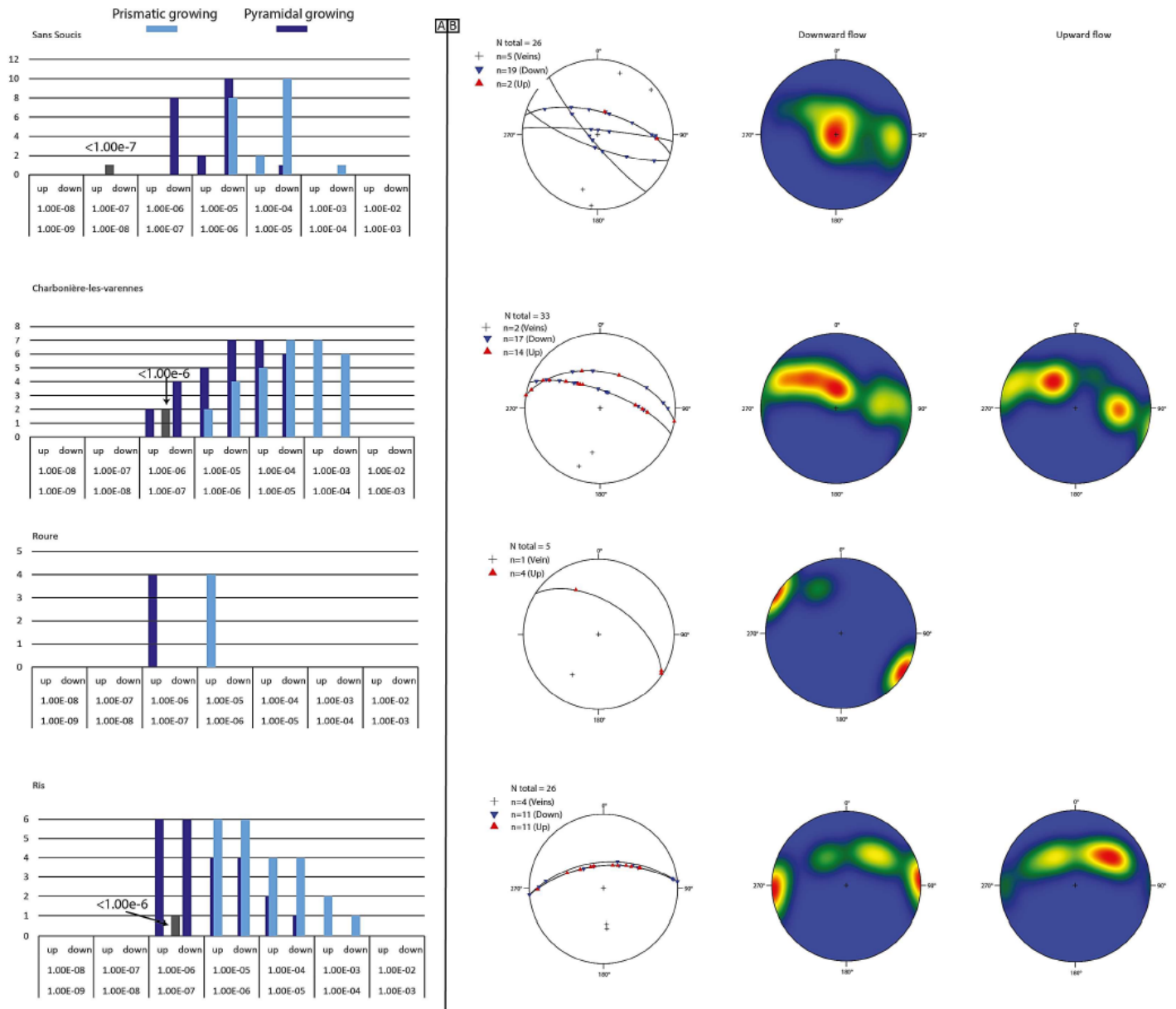


**Figure 4**

A. Direction and velocity of fluid flow for each area studied. B. Stereographic plot of the fluid flow directions deduced from growth band thickness relative to position (see text).

## Supplementary Files

This is a list of supplementary files associated with this preprint. Click to download.

- [Textesupdata.docx](#)
- [supdata1.pdf](#)
- [supdata2V2.pdf](#)